CrossMark

Decreasing monsoon precipitation in southwest China during the last 240 years associated with the warming of tropical ocean

Liangcheng Tan[1,2,3] · Yanjun Cai[1,2] · Zhisheng An[1,2] · Hai Cheng[2,4] ·
Chuan-Chou Shen[5] · Yongli Gao[6] · R. Lawrence Edwards[4]

Abstract Based on an absolutely dated stalagmite $\delta^{18}O$ record from Yunnan province, China, we reconstructed monsoon precipitation variations in southwest China since 1760 AD with a resolution of about 2 years. Combining the speleothem $\delta^{18}O$ and observed rainfall records, we find an overall decreasing trend in monsoon precipitation in this region and suggest that the recent drought in 2009–2012 AD has been the driest since 1760 AD. Our speleothem record is consistent with the monsoon precipitation records reconstructed from tree rings in the Nepal Himalaya and southeastern Tibetan Plateau. However, it is anti-correlated with a speleothem record from central India, which confirms the observed anti-phase variations of Indian monsoon precipitation with moistures from the Bay of Bengal and Arabian Sea on multi-decadal to centennial timescales during historical time. The long-term warming of tropical ocean may have caused the decrease of the land-sea thermal gradient and the amount of moisture transported from the Bay of Bengal, which may reduce precipitations in southwest China during the last 240 years. On decadal scale, El Niño-like conditions of tropical Pacific sea surface temperature may cause drought in this region. Climate model simulations suggest El Niño-like conditions exist in tropical Pacific under global warming scenarios. As a result, it is crucial to have adaptive strategies to overcome future declines in precipitation and/or drought events in southwest China.

Keywords Drought · Southwest China · Tropical SST · El Niño · Stalagmite

1 Introduction

Frequent occurrences of droughts in southwest China in recent years have raised increasing concerns among public and scientific communities (Wu 2011; Yin 2010). Due to limited storage capacity of soil water over the widely distributed karst landform in southwest China along with impacts of human activities, droughts have induced severe economic and social problems in recent years. For example, droughts in Yunnan province, southwest China during 2009–2012 AD have directly caused more than 7.3 billion US dollar of financial loss and threatened the life of many people (Tao et al. 2014).

Meteorologists (Barriopedro et al. 2012; Huang et al. 2011, 2012; Li et al. 2009; Zhang et al. 2011) suggested that droughts during rainy seasons were caused by the westward shift of enhanced Western Pacific Subtropical High (WPSH), which blocked the transfer of warm and humid moistures from the Bay of Bengal to southwest China. Meanwhile, the meridional water vapor flux from

✉ Liangcheng Tan
  tanlch@ieecas.cn

1 State Key Laboratory of Loess and Quaternary Geology, Institute of Earth Environment, Chinese Academy of Sciences, Xi'an 710061, China

2 Institute of Global Environmental Change, Xi'an Jiaotong University, Xi'an 710054, China

3 Joint Center for Global Change Studies (JCGCS), Beijing 100875, China

4 Department of Earth Sciences, University of Minnesota, Minneapolis, MN 55455, USA

5 High-Precision Mass Spectrometry and Environment Change Laboratory (HISPEC), Department of Geosciences, National Taiwan University, Taipei 106, Taiwan

6 Department of Geological Sciences, Center for Water Research, University of Texas at San Antonio, San Antonio, TX 78249, USA

🌀 Springer

the Bay of Bengal was weak. However, these analyses were based on short-term observations for the past 60 years and mainly focused on synoptic scale drought events. Only limited studies investigate decadal scale drought events based on tree ring records from the western margin of southwest China, i.e. southeastern Tibetan plateau (Fan et al. 2008; An et al. 2013; Bi et al. 2015). Decadal scale drought can cause much more damage to society, and even played an important role on the collapse of some Chinese dynasties (Zhang et al. 2008; Tan et al. 2011) and classic Maya civilization (Kennett et al. 2012; Medina-Elizalde and Rohling 2012).

A declining trend in monsoon precipitation was thought to exist in southwest China during the last 60 years (Zhang and Li 2014) along with frequent occurrences of extreme droughts (He et al. 2011). What's the driving force of the declined monsoon precipitation in the last 60 years? Was the recent decadal drought unprecedented? Will the reduced monsoon precipitation trend continue in the future? Answers to these important questions are crucial for water and resource management in southwest China.

In this paper, we reconstructed the monsoon precipitation variation history in southwest China during the past 240 years based on $\delta^{18}O$ records of a high-resolution, absolutely dated stalagmite from Yunnan province, southwest China. Variations and driving forces of monsoon precipitation in this region were further discussed.

2 Cave location and climatology

Xiaobailong Cave (N24°12′, E103°21′, 1500 m above sea level), located 20 km south of Mile, Yunnan, southwest China (Fig. 1), formed in Middle Triassic dolomitic limestone and calcite dolomite of the Gejiu Group. The cave, with a small entrance, is about 500 m long and the cave roof ranges from 20 to 60 m thick. The relative humidity is >90 % inside the cave (Cai et al. 2006), and cave air temperature is 17.2 °C, consistent with local mean annual temperature (17.3 °C, Cai et al. 2015). Annual precipitation in this region is 960 mm, and ~80 % occurs during summer monsoon months (June–September). Most of the water surplus occurs between July and October as calculated by the Thornthwaite evapotranspiration model (Thornthwaite 1948; McCabe and Markstrom 2007; Fig. 2). As a result, recharge of the aquifer in this area occurs mainly from summer monsoon rainfall. Previous work suggested that the regional precipitation is positively correlated with that in the northern Indo-China Peninsula (Cai et al. 2015). Water vapor of this region in rainy season mainly comes from the Bay of Bengal (Fig. 1) and is dominated by Indian summer monsoon.
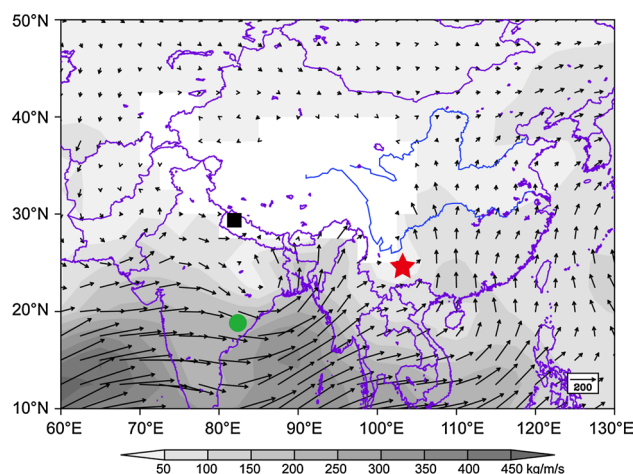
Fig. 1 Location of Xiaobailong Cave (*red star*) and moisture transport pathway. Rainy season (Jun.–Sep.) water vapor transport (kg m^{-1} s^{-1}) averaged for the period 1961–2012 at low level (700 hPa) based on the NCEP/NCAR reanalysis datasets (Kalnay et al. 1996), using the Grid Analysis and Display System (GrADS). The *shading* shows absolute value of water vapor transport at each grid. The *green solid circle* and *black solid square* represent Jhumar Cave from India (Sinha et al. 2011) and tree ring site from Nepal (Sano et al. 2012), respectively

By using various stalagmite records from Xiaobailong Cave, Cai et al. (2006, 2015) reconstructed millennial- to orbital-scales Indian monsoon precipitation variability over the past 252,000 years. Over orbital scale, monsoon precipitation in this region is dominated by 23-kyr precessional cycle. However, there are also clear glacial–interglacial variations, which are different from cave records from East China. On millennial scale, there is a clear link between monsoon precipitation and climate in the North Atlantic (Cai et al. 2015). In addition, climate of the high southern latitudes may also influence some millennial scale monsoon precipitation variations in this region (Cai et al. 2006).

3 Sample and methods

We collected a new stalagmite sample XBL41, 7.5 cm in length, in the inner chamber of the cave (about 400 m from the entrance) in November 2006. The top of the stalagmite was receiving drip water when collected, indicating possibly active growth. After halved and polished, the stalagmite section showed clear growth bandings. Two obvious growth hiatuses were observed at 0.5 and 6.0 cm of the stalagmite (Fig. 3). From the first hiatus to the topmost part, the lithology of the stalagmite changed from aragonite to calcite as identified by petrographic and X-ray Diffraction (XRD) analyses.

Ten subsamples (Fig. 3) were drilled and dated with U-series methods on a multi-collector inductively coupled

Fig. 2 Monthly mean precipitation (*gray bars*), temperature (*blue squares*), and water surplus (*red squares*) at the Kunming station, ~100 km northwest of Xiaobailong Cave (1957–2009 AD)
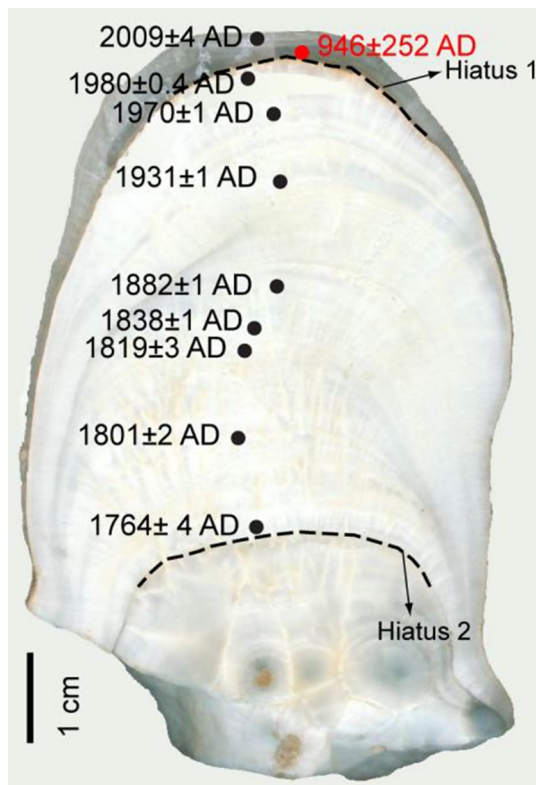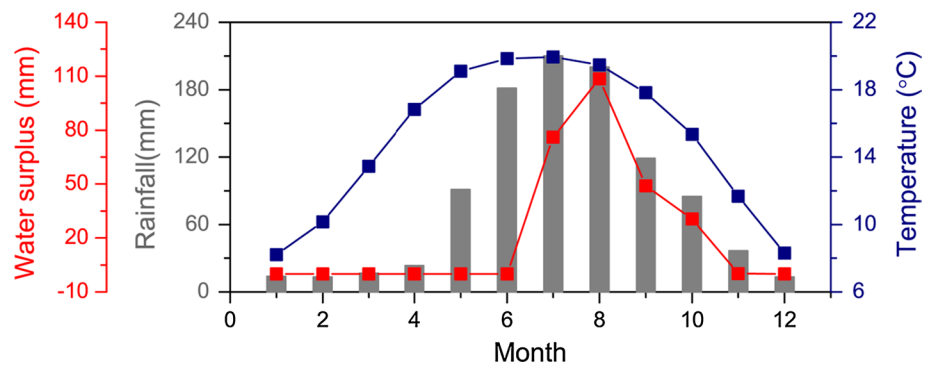
Fig. 3 Cross-section of XBL41 from Xiaobailong Cave. All ^{230}Th dating positions are *marked* on the stalagmite with 2σ errors. The *red dot* indicates an excluded dating subsample, which was contaminated. The *dashed lines* represent two growth hiatuses

plasma mass spectrometer (MC-ICPMS) at the University of Minnesota, USA and Xi'an Jiaotong University, China (Edwards et al. 1987; Shen et al. 2003; Cheng et al. 2013). An initial ^{230}Th/^{232}Th atomic ratio of $4.4 \pm 2.2 \times 10^{-6}$ were used to correct for initial ^{230}Th amount. Subsamples for stable isotope analyses were drilled out at intervals of 0.5 mm. Seven coeval subsamples from two layers, respectively, were selected for the "Hendy test" (Hendy 1971) to evaluate the isotopic equilibrium during mineral precipitation. Stable isotope analyses were performed on a Finnigan MAT-252

mass spectrometer equipped with a Kiel III Carbonate Device at the Institute of Earth Environment, Chinese Academy of Sciences. The replicates showed that the precision of δ^{18}O analysis is better than ±0.06 ‰ (2σ, VPDB).

4 Results

4.1 Chronology

Table 1 shows ^{230}Th dating results. All the subsamples measured are in stratigraphic order, except for the date of XBL41-7. This subsample contains high detrital ^{232}Th levels (2.1×10^4 ppt) and large dating uncertainties (±252 years, Table 1), which was contaminated by high detrital ^{232}Th in the hiatus layer. The layer XBL41-7 was excluded from the established age model. A linear interpolation model was used to establish the chronology of XBL41 (Fig. 4). The result indicates that the top 6 cm part of the stalagmite grew from 1760 AD to the present (2006 AD, the time of sampling), with a short hiatus occurred after 1981 AD.

As we are unable to confirm the accurate duration of the hiatus, the period of 1760–1981 AD was selected for this study. The corrections for the initial ^{230}Th were negligible because of high ^{238}U concentrations (11–31 ppm) and the low ^{232}Th levels (11–300 ppt) in the subsamples (Table 1). Most of the absolute dating errors were ±1–2 years. The growth rates of XBL41 range from 0.11 to 0.37 mm/year (Fig. 4).

4.2 δ^{18}O record

The δ^{18}O values of XBL41 vary between -8.8 and -11.0 ‰ with an average value of -9.7 ‰. During the last 240 years, the δ^{18}O record shows progressively increasing trend. The δ^{18}O values increased about 2.2 ‰ from 1760 to 1850 AD, followed by a decrease of 1.1 ‰ in the next 20 years. Since 1870 AD, the δ^{18}O values increased again, with a trend of about 1.6 ‰ towards heavy δ^{18}O (Fig. 5).

Table 1 U-Th isotopic data and ^{230}Th dates of stalagmite XBL41

Sample ID	Depth (cm)	^{238}U (ppb)	^{232}Th (ppt)	^{230}Th/^{232}Th (atomic × 10^{-6})	^{230}Th/^{238}U (activity)	δ^{234}U (measured)	^{230}Th Age (year; uncorrected)	^{230}Th Age (year BP; corrected)	^{230}Th Age (year AD; corrected)	δ^{234}U$_{initial}$ (corrected)
XBL41-1	5.75	18,167 ± 71	77 ± 6	9468 ± 736	0.00242 ± 0.00004	86.1 ± 2.1	243 ± 4	186 ± 4	1764 ± 4	86.2 ± 2.1
XBL41-2	4.4	11,569 ± 28	256 ± 6	1524 ± 36	0.00204 ± 0.00002	78.1 ± 2.2	207 ± 2	149 ± 2	1801 ± 2	78.2 ± 2.2
XBL41-3	3.8	11,445 ± 37	200 ± 5	1800 ± 53	0.00191 ± 0.00003	63.3 ± 2.0	196 ± 3	132 ± 3	1819 ± 3	63.3 ± 2.0
XBL41-2A	3.65	16,925 ± 56	216 ± 5	2245 ± 55	0.00174 ± 0.00001	67.1 ± 1.9	178 ± 1	112 ± 1	1838 ± 1	67.1 ± 1.9
XBL41-4	2.95	13,094 ± 30	32 ± 6	8157 ± 1432	0.00122 ± 0.00001	65.3 ± 2.0	125 ± 1	112 ± 1	1882 ± 1	65.3 ± 2.0
XBL41-1A	1.8	27,235 ± 143	292 ± 8	1254 ± 40	0.00082 ± 0.00001	58.9 ± 2.5	84 ± 1	68 ± 1	1931 ± 1	58.9 ± 2.5
XBL41-5	0.95	26,949 ± 77	11 ± 6	14,261 ± 7241	0.00036 ± 0.00001	62.5 ± 2.2	37 ± 1	19 ± 1	1970 ± 1	62.5 ± 2.2
XBL41-6	0.65	31,462 ± 255	197 ± 4	782 ± 19	0.00030 ± 0.000004	67.6 ± 3.8	30 ± 0.4	−30 ± 0.4	1980 ± 0.4	67.7 ± 3.8
XBL41-7	0.4	1606 ± 2	20,684 ± 415	18 ± 0.4	0.01369 ± 0.0001	55.1 ± 1.6	1423 ± 13	1004 ± 252	946 ± 252	55.3 ± 1.6
XBL41-8	0.1	4002 ± 14	135 ± 4	−3 ± 17	−0.00001 ± 0.00004	57.6 ± 2.2	−1 ± 4	−59 ± 4	2009 ± 4	57.6 ± 2.2

The errors are 2σ errors. Decay constant values are: $\lambda_{230} = 9.1705 \times 10^{-6}$/a, $\lambda_{234} = 2.82206 \times 10^{-6}$/a (Cheng et al. 2013) and $\lambda_{238} = 1.55125 \times 10^{-10}$ year^{-1} (Jaffey et al. 1971). Corrected ^{230}Th ages assume the initial ^{230}Th/^{232}Th atomic ratio of 4.4 ± 2.2 × 10^{-6}. Depths along the growth axes are relative to the top (youngest surface) of the stalagmite. Year BP: year before present (1950 AD). XBL41-1A and XBL41-2A were dated at Xi'an Jiaotong University, China. The other subsamples were dated at the University of Minnesota, USA

5 Discussion

5.1 Climate significance of stalagmite δ^{18}O

"Hendy test" results show that the δ^{18}O values remain constant along the two growth layers of XBL41 (Fig. 6), suggesting it was most likely deposited at isotopic equilibrium fractionation conditions (Hendy 1971). Both cave temperature (close to surface annual mean temperature) and the δ^{18}O in precipitation can affect the δ^{18}O of stalagmite under isotopic equilibrium fractionation conditions. Temperature-dependent fractionation change [oxygen isotope fractionation of aragonite-water is $10^3 \ln\alpha = (17.88 \pm 0.13) \times 10^3$ /T − (31.14 ± 0.46); (Kim et al. 2007)] should not be the dominant factor controlling the stalagmite δ^{18}O variations in this study. Otherwise, low temperatures in the cold Little Ice Age (15th–19th centuries (Ge et al. 2013) would enhance δ^{18}O values, which is opposite to our δ^{18}O record (Fig. 5).

Rainfall amount, moisture recycling and circulation, and changes in moisture source and transport pathway may affect the δ^{18}O in precipitation (Breitenbach et al. 2010; Cai et al. 2010; Tan 2014). Recently, Cai et al. (2015) suggested that there were similar 850-hPa wind trajectories for both present day and Last Glacial Maximum in Xiaobailong Cave site, indicating the moisture paths from the Bay of Bengal to Xiaobailong Cave were relatively stable even on millennial- to orbital-timescales. In addition, the impact of seawater δ^{18}O of the Indian Ocean and the Pacific Ocean on the precipitation δ^{18}O is negligible compared with the rather large magnitude of inter-annual variations in precipitation δ^{18}O (Tan 2014). The distance from Xiaobailong Cave to the Bay of Bengal is similar to the distance from the other potential moisture source-South China Sea in modern condition, which reduces the impacts of changes in moisture source and transport pathway (Tan et al. 2015).

Recently, a simulation result indicated a significant negative correlation between the precipitation δ^{18}O and monsoon rainfall amount in southwest China (Liu et al. 2014). To further confirm the climate significance of our stalagmite δ^{18}O, we directly compare the XBL41 δ^{18}O record with the observed annual rainfall (mainly contributed by monsoonal rainfall) record. Because of the short overlapping period (~30 years, 1951–1981 AD), different resolution and the age uncertainties of XBL41 record, it is hard to get a significant correlation coefficient between the two series. However, the two series are consistent from sub-decadal- to decadal-timescales. For example, the relative dry periods in the early 1950s and the late 1960s and 1970s corresponded to higher δ^{18}O values. In contrast, the relative wet periods in the early 1970s and middle 1960s corresponded to lower δ^{18}O within age errors (Fig. 5). The
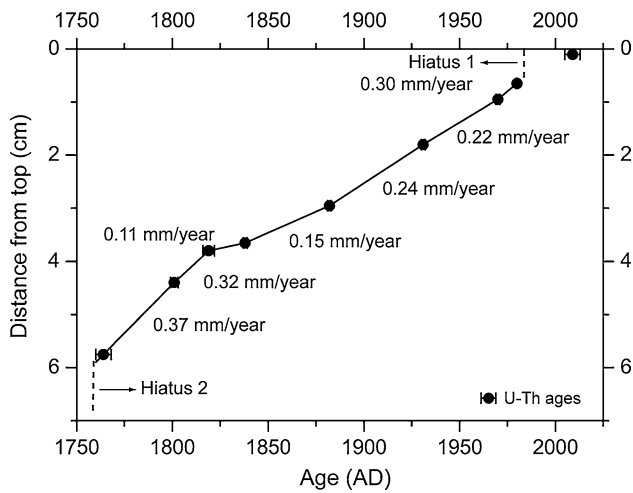
Fig. 4 Plot of age verses depth for XBL41. *Error bars* indicate ^{230}Th dates with 2σ errors. Growth rates of the stalagmite range from 0.11 to 0.37 mm/year
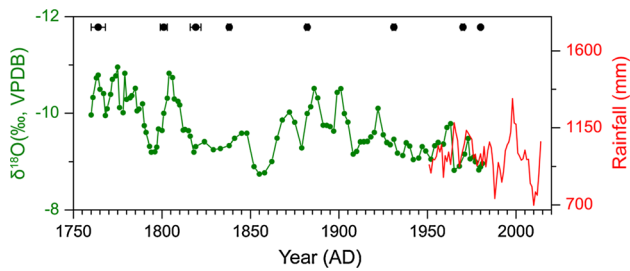

Fig. 5 XBL41 δ^{18}O record during 1760–1981 AD (*solid circle*) and its comparison with annual precipitation (*red line*, 3-point moving average) record from Kunming meteorological station
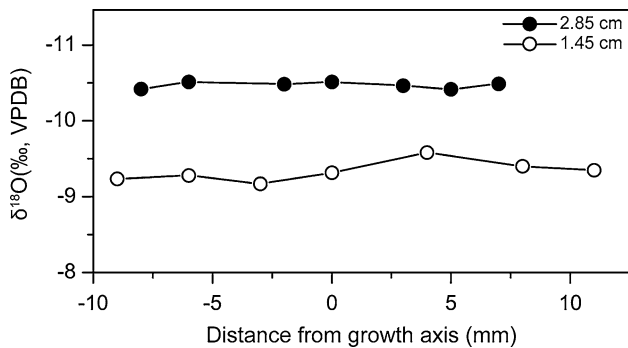
Fig. 6 Hendy test on two horizons of stalagmite XBL41

correspondence confirms the robust anti-phase relationship between the speleothem/precipitation δ^{18}O and monsoon rainfall amount in southwest China (Liu et al. 2014). As a result, the XBL41 δ^{18}O record reflects Indian monsoon precipitation changes in southwest China during the last 240 years.
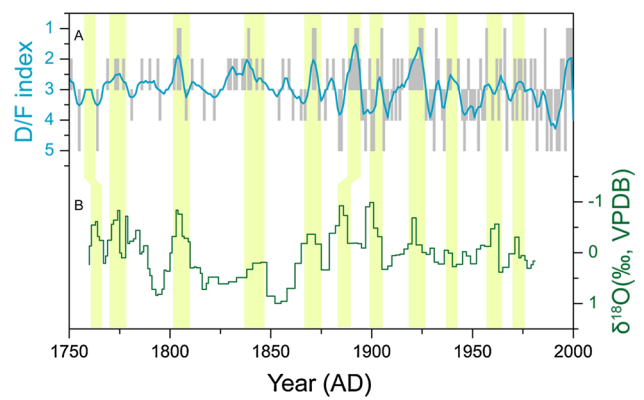
Fig. 7 Comparison between (*a*) historical Drought/Flood (D/F) index record from Kunming (CAMS 1981) and (*b*) detrended XBL41 δ^{18}O record. The *yellow bars highlight* the periods of decreased stalagmite δ^{18}O values and D/F index

5.2 Indian monsoon precipitation variations in southwest China during the last 240 years

Our stalagmite δ^{18}O record also corresponds well with a moisture record (Drought/Flood index) reconstructed from historical documents in Kunming station (CAMS 1981). Because Drought/Flood (D/F) index was defined by the method of 5-level classification, it can hardly reflect the long-term trend of rainfall variations. As a result, we compare the detrended δ^{18}O record with the D/F index record. As shown in Fig. 7, the decadal scale variations of the stalagmite record were also recorded in the D/F index series. For example, both series recorded the wet periods in the 1770s, 1800s, 1870s and the early 1900 and 1920s.

In general, our stalagmite δ^{18}O result suggests that the Indian monsoon precipitation in southwest China gradually decreased in the last 240 years. The first decreasing period is from 1760 AD to 1850 AD, and the second remarkable decreasing period is from the late 19th century to present (1981 AD). The drying rate in the last century was slower than that in the period of 1760–1850 AD. Notable decadal- and sub-decadal scale droughts were identified in the 1790s, 1820s, 1850s, early 1910s and 1940s in historical time (Fig. 5).

The decreasing precipitation trend in the last 240 years is consistent with the declined lake level of Chenghai Lake in the northwest Yunnan province. Historical document recorded that the Chenghai Lake was an open lake before 1779 AD, and after that, it was closed (Xu et al. 2015). Some of the exposed lake terraces were dated in the Little Ice Age (Xu H. unpublished data), further supporting a higher than present lake level at that time. By combining the speleothem δ^{18}O record with the observed rainfall record, our result indicates that the drought during 2009–2012 AD was the driest since 1760 AD (Fig. 5). The

drought occurred along the long-term drying trend, which means it was extremely severe.

5.3 Dipolar structure of Indian monsoon precipitation during historical time

Meteorological observation records indicate that the trends of the Indian monsoon rainfall over different regions are different during the last hundred years (Guhathakurta and Rajeevan 2008; Mishra et al. 2012). The region south of 20°N, receiving moisture from the Arabian Sea shows an increasing rainfall trend in monsoon season. On the contrary, northeastern India, which receives moisture from the Bay of Bengal, shows a decreasing rainfall trend (Guhathakurta and Rajeevan 2008; Konwar et al. 2012; Mishra et al. 2012). Recently, a stalagmite, JHU-1, from central India with decreasing δ^{18}O values since the late 17th century, demonstrates a shift towards enhanced monsoon precipitation in this region. In contrast, increasing δ^{18}O values were observed in a stalagmite, WS-B, from northeastern India during this period, indicating declined regional monsoon precipitation (Sinha et al. 2011). Moreover, a 2000-years long stalagmite δ^{18}O record from northwestern India, where both receive moistures from the Arabian Sea and the Bay of Bengal, shown both similarities and discrepancies with the JHU-1 record from central India (Sinha et al. 2015). Therefore, it is crucial to confirm the dipolar structure of the precipitation of the two branches of Indian monsoon, as well as its temporal and spatial extension during historical time. Because there is no age control in the last 200 years of the WS-B record from northeastern India, more evidences are needed.

In this paper, XBL41 record is compared with the JHU-1 record from central India. As shown in Fig. 8, an anti-phase relationship of the two records was observed during the last 240 years. The increasing trends of XBL41 δ^{18}O values during the periods of 1760–1850 AD and from the late 19th century to present correspond to the decreasing trends of JHU-1 δ^{18}O records during these periods (Fig. 8). From 1850 to 1870 AD, the XBL41 δ^{18}O values abruptly decreased, while the JHU-1 δ^{18}O values increased drastically. Tree ring δ^{18}O reconstructed monsoon precipitation in Nepal Himalaya (Sano et al. 2012), with moisture source from the Bay of Bengal, shows similar variations with the XBL41 δ^{18}O record (Fig. 8). Declining monsoon precipitation was observed in the tree ring δ^{18}O records from southern (Griebinger et al. 2011) and southeastern part of Tibetan Plateau (Wernicke et al. 2015) too. In addition, the long-term trend of the XBL41 record is consistent with that of the South Asia summer monsoon (e.g. Indian monsoon) index record (Shi et al. 2014), since the monsoon rainfall variability, with moisture from the Bay of Bengal, can well represent the Indian summer monsoon intensity variability (Gadgil 2003).
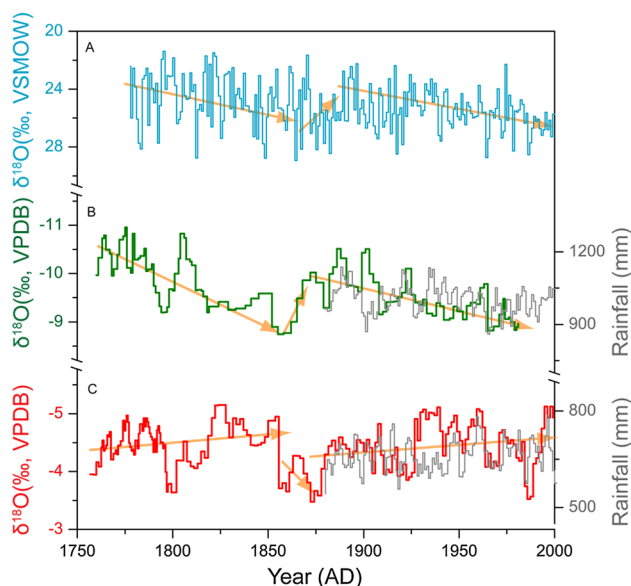

Fig. 8 Comparisons of (*a*) tree ring δ^{18}O record from Nepal Himalaya (Sano et al. 2012), (*b*) stalagmite XBL41 δ^{18}O record from southwest China, and (*c*) stalagmite JHU-1 δ^{18}O record from central India (Sinha et al. 2011). The *dark yellow arrows* represent the linear trends of different periods in the three records, respectively. The *gray lines* in panels *b* and *c* are observed monsoon rainfall records (3-point moving average) of central northeast India and peninsular India during 1880–2000 AD, respectively (data comes from Indian Institute of Tropical Meteorology). Observed records also show long-term regional differences in Indian monsoon rainfalls during the last century

In summary, comparisons of the XBL41 record with other paleoclimate records in the region confirm the observed dipolar structure of Indian monsoon precipitation variability (Konwar et al. 2012; Mishra et al. 2012) on multi-decadal- to centennial- scales during historical time.

5.4 Controlling factors of Indian monsoon precipitation in southwest China

Many studies suggested that the tropical sea surface temperature (SST) variations have important influences on the spatial–temporal variations of Asian monsoon rainfall (Wang 2006). In particular, the ENSO's impact on the Indian monsoon circulation has been studied extensively (Berkelhammer et al. 2014; Cherchi and Navarra 2013; Mishra et al. 2012; Park et al. 2010; Webster et al. 1998). It was evident that the teleconnection between ISM precipitation and ENSO has undergone a protracted weakening since the late 1980s (Kumar et al. 1999). As a notable example, the 1997/1998 El Niño event, despite its intensity, produced only marginal rainfall anomalies over India (Kucharski et al. 2007). However, Chen and Yoon (2000) demonstrated that ENSO could significantly influence the moisture conditions over Indo-china on inter-annual timescale. Buckley
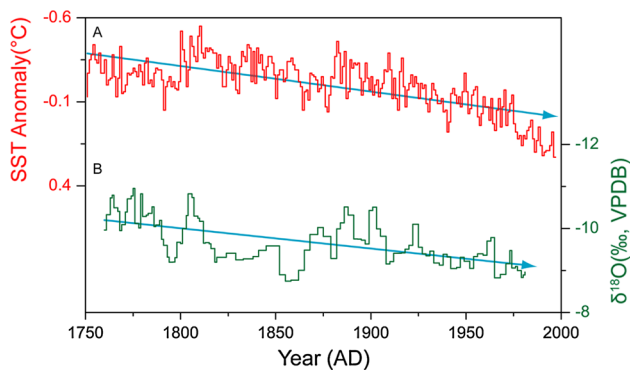
Fig. 9 Comparison between (*b*) stalagmite XBL41 δ^{18}O record and (*a*) tropical Indo-Pacific ocean SST anomaly (Wilson et al. 2006). The blue arrows in *a* and *b* represent the linear trends of the two records

et al. (2007) also suggested that ENSO might be the major contributing factor to decadal scale drought over northwestern Thailand. Ummenhofer et al. (2013) stated that the drought patterns across monsoon and temperate Asia over the period 1877–2005 were linked to Indo-Pacific climate variability associated with the ENSO and the Indian Ocean Dipole (IOD). Recently, Zhang et al. (2013) suggested that the drought in southwest China during autumn 2009 was caused by a nonconventional El Niño, with the maximum SST anomalies confined to the central equatorial Pacific Ocean. The XBL41 record also demonstrated the influence of tropical ocean SST and ENSO on the monsoon precipitation in southwest China during the last 240 years.

As show in Fig. 9, there is a long-term increasing trend of tropical Indo-pacific Ocean SST during the last two century (Wilson et al. 2006). Meanwhile, the increase of temperature in continent where the Indian low pressure develops may be smaller than that over the sea surface, which was resulted from increasing aerosol cooling effect and shrinking Himalayan snow cover (Ramanathan et al. 2005; Zhao and Moore 2006; Xu et al. 2012). The decreasing land-sea thermal gradient may reduce the moisture transport from the Bay of Bengal and cause the long-term decreasing of rainfall in southwest China.

The low-level cross-equatorial flow in the western Indian Ocean is an essential component of the Indian summer monsoon (Wang 2006). Compared to that of the Bay of Bengal, the major contribution for the moisture fluxes to the Arabian Sea comes from the southern Indian Ocean brought by the cross-equatorial flow (Kumar et al. 1999). A marine record from northwest Arabian Sea reveals intensified upwelling in the last 240 years (Anderson et al. 2002), indicating strengthening northward cross-equatorial moisture transport. The intensified northward cross-equatorial moisture transport could enhance the monsoon rainfall in peninsular and west central India (Puranik et al. 2014;
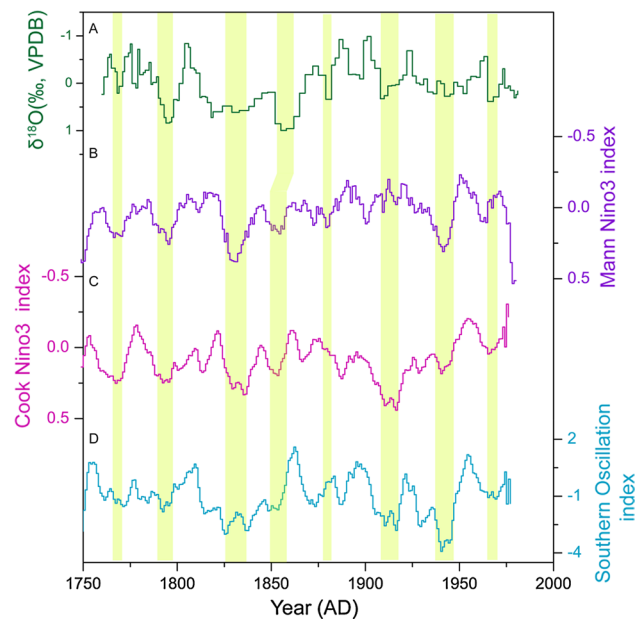
Fig. 10 Comparisons of (*a*) detrended XBL41 δ^{18}O record with (*b*) Nino3 index record (10-point moving smooth, Mann Nino3 index) reconstructed by Mann et al. (2000), (*c*) Nino3 index record (10-point moving smooth, Cook Nino3 index) reconstructed by D'Arrigo et al. (2005), and (*d*) Southern Oscillation index series (10-point moving smooth, Stahle et al. 1998). The *shaded yellow bars* indicate drought events in southwest China and their correlation with various series

Sinha et al. 2011). Modern observation data indicate the low level wind speed and moisture transport over the Arabian Sea increased, which caused increased rainfall in peninsular and west central India during the last 30 years. In contrast, decreasing trends of low level wind speed and moisture transport from the Bay of Bengal were observed (Konwar et al. 2012). The observation further supports our explanation.

On decadal timescale, the detrended XBL41 record shows similar patterns to the Nino3 SST reconstructions (D'Arrigo et al. 2005; Mann et al. 2000), as well as the Southern Oscillation index series (Stahle et al. 1998), despite some discrepancies among the different proxy reconstructions (Fig. 10). The Person correlation coefficient between XBL41 record and the Nino3 index record (10-point moving smooth) reconstructed by Mann et al. (2000) is 0.29 ($p < 0.05$). A significant negative correlation coefficient ($r = -0.28$, $p < 0.05$) was also observed between XBL41 record and the Southern Oscillation Index series (10-point moving smooth, Stahle et al. 1998). The comparisons suggest that the decadal variability of east Pacific SST significantly influences the monsoon rainfall in southwest China. In decadal El Niño-like conditions, droughts occurred in southwest China. In contrast, enhanced monsoon rainfall in southwest China corresponded to decadal La Niña-like conditions (Fig. 10). Tropical Pacific SST's

impact on the monsoon rainfall in southwest China was thought to be related to the east–west displacement of the ascending and descending branches of the Walker circulation (Ropelewski and Halpert 1987). The abnormal ocean warming during El Niño-like conditions may cause the ascending branch of Walker circulation move eastward. As a result, the descending branch broadly distributed over northeast India and southwest China, suppressing monsoon rainfalls in these regions (Kumar et al. 2006; Ropelewski and Halpert 1987).

It was observed that at annual scale, the inverse relationship between the El Niño events with the warmest SSTs in the eastern equatorial Pacific and the Indian monsoon rainfall broke down in recent decades (Kumar et al. 1999). In contrast, the El Niño events with the warmest SST anomalies in the central equatorial Pacific are more effective in forcing drought and producing subsidence over India (Kumar et al. 2006; Ratnam et al. 2010; Wang et al. 2015). However, there are similar variations (r = 0.97, N = 707, $p < 0.01$) in SST of eastern and central equatorial Pacific in the long term (1300–2006 AD, Cook et al. 2008). Climate model simulation results suggest that the tropical Pacific SST gradient will decrease under conditions of global warming, resembling El Niño-like SST patterns (An et al. 2012; Liu et al. 2013). Multi model ensembles of CMIP3 and CMIP5 also show consistently weak and eastward shift of the Walker Circulation along the equator under global warming condition (Bayr et al. 2014). Consequently, there might be a decreasing trend of monsoon precipitation in southwest China under the El Niño-like conditions under the scenario of global warming in the future. Therefore, it is crucial to come up with adaptive strategies to prepare for potential declines of precipitation and/or drought events in southwest China in the future.

6 Conclusions

1. The high-resolution δ^{18}O record of an absolutely dated stalagmite from Xiaobailong Cave in Yunnan province, China reveals an overall decreasing trend in monsoon precipitation in southwest China during the last 240 years. By combining the speleothem δ^{18}O with the observed rainfall record, we suggested that the recent drought in 2009–2012 AD was the driest since 1760 AD. The drought occurred in a long-term drying trend, which means it is extremely severe.

2. Our speleothem record is consistent with monsoon precipitation records in Nepal Himalaya and southeastern Tibetan Plateau reconstructed from tree rings but anticorrelated with a speleothem record from central India. The comparisons confirm the observed anti-phase variations of Indian monsoon precipitation with moisture

sources from the Bay of Bengal and Arabian Sea on multi-decadal to centennial- timescales during historical time.

3. On centennial scale, the warming of the tropical ocean during the last 240 years may have decreased the land-sea thermal gradient and reduced the moisture transport from the Bay of Bengal, therefore reduced the monsoon rainfalls in southwest China. On decadal scale, El Niño-like conditions of east Pacific SST may also have significant influences on droughts in southwest China.

References

An S, Kim JW, Im S, Kim B, Park J (2012) Recent and future sea surface temperature trends in tropical Pacific warm pool and cold tongue regions. Clim Dyn 39:1373–1383. doi:10.1007/s00382-011-1129-7

An W, Liu X, Leavitt SW, Xu G, Zeng X, Wang W, Qin D, Ren J (2013) Relative humidity history on the Batang–Litang Plateau of western China since 1755 reconstructed from tree-ring δ^{18}O and δD data. Clim Dyn 42:2639–2654. doi:10.1007/s00382-013-1937-z

Anderson DM, Overpeck JT, Gupta AK (2002) Increase in the Asian southwest monsoon during the past four centuries. Science 297:596–599. doi:10.1126/science.1072881

Barriopedro D, Gouveia CM, Trigo RM, Wang L (2012) The 2009/10 drought in China: possible causes and impacts on vegetation. J Hydrometeorol 13:1251–1267. doi:10.1175/JHM-D-11-074.1

Bayr T, Dommenget D, Martin T, Power SB (2014) The eastward shift of the Walker Circulation in response to global warming and its relationship to ENSO variability. Clim Dyn 43:2747–2763. doi:10.1007/s00382-014-2091-y

Berkelhammer M, Sinha A, Mudelsee M, Cheng H, Yoshimura K, Biswas J (2014) On the low-frequency component of the ENSO-Indian monsoon relationship: a paired proxy perspective. Clim Past 10:733–744. doi:10.5194/cp-10-733-2014

Bi Y, Xu J, Gebrekirstos A, Guo L, Zhao M, Liang E, Yang X (2015) Assessing drought variability since 1650 AD from tree-rings on the Jade Dragon Snow Mountain, southwest China. Int J Climatol 35:4057–4065. doi:10.1002/joc.4264

Breitenbach SF, Adkins JF, Meyer H, Marwan N, Kumar KK, Haug GH (2010) Strong influence of water vapor source dynamics on stable isotopes in precipitation observed in southern Meghalaya, NE India. Earth Planet Sci Lett 292:212–220. doi:10.1016/j.epsl.2010.01.038

Buckley BM, Palakit K, Duangsathaporn K, Sanguantham P, Prasomsin P (2007) Decadal scale droughts over northwestern Thailand over the past 448 years: links to the tropical Pacific and Indian Ocean sectors. Clim Dyn 29:63–71. doi:10.1007/s00382-007-0225-1

Cai Y, An Z, Cheng H, Edwards RL, Kelly MJ, Liu W, Wang X, Shen CC (2006) High-resolution absolute-dated Indian Monsoon record between 53 and 36 ka from Xiaobailong Cave, southwestern China. Geology 34:621–624. doi:10.1130/G22567.1

Cai Y, Tan L, Cheng H, An Z, Edwards RL, Kelly MJ, Kong X, Wang X (2010) The variation of summer monsoon precipitation in central China since the last deglaciation. Earth Planet Sci Lett 291:21–31. doi:10.1016/j.epsl.2009.12.039

Cai Y, Fung IY, Edwards RL, An Z, Cheng H, Lee JE, Tan L, Shen CC, Wang X, Day JA (2015) Variability of stalagmite-inferred Indian monsoon precipitation over the past 252,000 y. Proc Natl Acad Sci 112:2954–2959. doi:10.1073/pnas.1424035112

Chen TC, Yoon JH (2000) Interannual variation in Indochina summer monsoon rainfall: possible mechanism. J Clim 13:1979–1986. doi:10.1175/1520-0442(2000)013<1979:IVIISM>2.0.CO;2

Cheng H, Edwards RL, Shen CC, Polyak VJ, Asmerom Y, Woodhead J, Hellstrom J, Wang Y, Kong X, Spötl C (2013) Improvements in 230Th dating, 230Th and 234U half-life values, and U-Th isotopic measurements by multi-collector inductively coupled plasma mass spectrometry. Earth Planet Sci Lett 371:82–91. doi:10.1016/j.epsl.2013.04.006

Cherchi A, Navarra A (2013) Influence of ENSO and of the Indian Ocean dipole on the Indian summer monsoon variability. Clim Dyn 41:81–103. doi:10.1007/s00382-012-1602-y

Chinese Academy of Meteorological Sciences (CAMS) (1981) Yearly charts of drought/flood in China for the last 500-year period. SinoMaps Press, Beijing

Cook ER, D'Arrigo RD, Anchukaitis KJ (2008) ENSO reconstructions from long tree-ring chronologies: Unifying the differences? Special workshop on "Reconciling ENSO Chronologies for the Past 500 Years", Moorea, French Polynesia

D'Arrigo R, Cook ER, Wilson RJ, Allan R, Mann ME (2005) On the variability of ENSO over the past six centuries. Geophys Res Lett 32:L03711. doi:10.1029/2004GL022055

Edwards RL, Chen JH, Wasserburg GJ (1987) 238U–234U–230Th–232Th systematic and the precise measurement of time over the past 500,000 years. Earth Planet Sci Lett 81:175–192. doi:10.1016/0012-821X(87)90154-3

Fan ZX, Braeuning A, Cao KF (2008) Tree-ring based drought reconstruction in the central Hengduan Mountains (China) since A.D. 1655. Int J Climatol 28:1879–1887. doi:10.1002/joc.1689

Gadgil S (2003) The Indian monsoon and its variability. Annu Rev Earth Planet Sci 31:429–467. doi:10.1146/annurev.earth.31.100901.141251

Ge Q, Hao Z, Zheng J, Shao X (2013) Temperature changes over the past 2000 year in China and comparison with the Northern Hemisphere. Clim Past 9:1153–1160. doi:10.5194/cp-9-1153-2013

Griebinger J, Brauning A, Helle G, Thomas A, Schleser G (2011) Late Holocene Asian summer monsoon variability reflected by δ18O in tree-rings from Tibetan junipers. Geophys Res Lett 38:L03701. doi:10.1029/2010GL045988

Guhathakurta P, Rajeevan M (2008) Trends in the rainfall pattern over India. Int J Climatol 28:1453–1469. doi:10.1002/joc.1640

He J, Zhang M, Wang P, Wang S, Wang X (2011) Climate characteristics of the extreme drought events in southwest China during recent 50 years. Acta Geogr Sin 66:1179–1190

Hendy CH (1971) The isotope geochemistry of speleothems: I. The calculation of the effects of different modes of formation on the isotopic composition of speleothems and their applicability as paleoclimate indicators. Geochim Cosmochim Acta 35:801–824. doi:10.1016/0016-7037(71)90127-X

Huang H, Li Q, Gao Y, Zhong A, Chen H, Li J (2011) Diagnosis of the severe drought in autumn/winter 2009–2010 in Yunnan province. Trop Geogr 31:28–31

Huang R, Liu Y, Wang L, Wang L (2012) Analyses of the cause of severe drought occurring in southwest China from the fall of 2009 to the spring of 2010. Chin J Atmos Sci 36:443–457. doi:10.3878/j.issn.1006-9895.2011.11101

Jaffey AHK, Flynn F, Glendenin LE, Bentley WC, Essling AM (1971) Precision measurement of half-lives and specific activities of 235U and 238U. Phys Rev C 4:1889–1906. doi:10.1103/PhysRevC.4.1889

Kalnay E, Kanamitsu M, Kistler R, Collins W, Deaven D, Gandin L, Iredell M, Saha S, White G, Woollen J (1996) The NCEP/NCAR 40-year reanalysis project. B Am Meteorol Soc 77:437–471. doi:10.1175/1520-0477(1996)077<0437:TNYRP>2.0.CO;2

Kennett DJ, Breitenbach SF, Aquino VV, Asmerom Y, Awe J, Baldini JU, Bartlein P, Culleton BJ, Ebert C, Jazwa C (2012) Development and disintegration of Maya political systems in response to climate change. Science 338:788–791. doi:10.1126/science.1226299

Kim ST, O'Neil JR, Hillaire-Marcel C, Mucci A (2007) Oxygen isotope fractionation between synthetic aragonite and water: influence of temperature and M_g^{2+} concentration. Geochim Cosmochim Acta 71:4704–4715. doi:10.1016/j.gca.2007.04.019

Konwar M, Parekh A, Goswami B (2012) Dynamics of east-west asymmetry of Indian summer monsoon rainfall trends in recent decades. Geophys Res Lett. doi:10.1029/2012GL052018

Kucharski F, Bracco A, Yoo J, Molteni F (2007) Low-frequency variability of the Indian monsoon-ENSO relationship and the tropical Atlantic: The "weakening" of the 1980 s and 1990s. J Clim 20:4255–4266. doi:10.1175/JCLI4254.1

Kumar KK, Rajagopalan B, Cane MA (1999) On the weakening relationship between the Indian monsoon and ENSO. Science 284:2156–2159. doi:10.1126/science.284.5423.2156

Kumar KK, Rajagopalan B, Hoerling M, Bates G, Cane M (2006) Unraveling the mystery of Indian monsoon failure during El Nino. Science 314:115–119. doi:10.1126/science.1131152

Li Y, Xu H, Liu D (2009) Feature of the extermely severe drought in the east of Southwest China and anomalies of atmospheric circulation in summer 2006. Acta Meteorol Sin 67:122–132. doi:10.1007/s13351-011-0025-8

Liu J, Wang B, Cane MA, Yim SY, Lee JY (2013) Divergent global precipitation changes induced by natural versus anthropogenic forcing. Nature 493:656–659. doi:10.1038/nature11784

Liu ZY, Wen XY, Brady EC, Otto-Bliesner B, Yu G, Lu HY, Cheng H, Wang YJ, Zheng WP, Ding YH, Edwards RL, Cheng J, Liu W, Yang H (2014) Chinese cave records and the East Asia summer monsoon. Quat Sci Rev 83:115–128. doi:10.1016/j.quascirev.2013.10.021

Mann ME, Gille EP, Bradley RS, Hughes MK, Overpeck JT, Keimig FT, Gross WS (2000) Global temperature patterns in past centuries: an interactive presentation. Earth Interact 4:1–29. doi:10.1175/1087-3562(2000)0042.3.CO;2

McCabe GJ, Markstrom SL (2007) A monthly water-balance driven by a graphical user interface. US Geological Survey Open-File Report 2007–1088, p 6

Medina-Elizalde M, Rohling EJ (2012) Collapse of classic Maya civilization related to modest reduction in precipitation. Science 335:956–959. doi:10.1126/science.1216629

Mishra V, Smoliak BV, Lettenmaier DP, Wallace JM (2012) A prominent pattern of year-to-year variability in Indian summer monsoon rainfall. Proc Natl Acad Sci 109:7213–7217. doi:10.1073/pnas.1119150109

Park HS, Chiang JC, Lintner BR, Zhang GJ (2010) The delayed effect of major El Nino events on Indian monsoon rainfall. J Clim 23:932–946. doi:10.1175/2009JCLI2916.1

Puranik SS, Ray K, Sen P, Kumar PP (2014) Impact of cross-equatorial meridional transport on the performance of the southwest monsoon over India. Curr Sci India 107:1006–1013

Ramanathan V, Chung C, Kim D, Bettge T, Buja L, Kiehl JT, Washington WM, Fu Q, Sikka DR, Wild M (2005) Atmospheric

brown clouds: impacts on South Asian climate and hydrological cycle. Proc Natl Acad Sci 102:5326–5333. doi:10.1073/pnas.0500656102

Ratnam JV, Behera SK, Masumoto Y, Takahashi K, Yamagata T (2010) Pacific Ocean origin for the 2009 Indian summer monsoon failure. Geophys Res Lett 37:L07807. doi:10.1029/2010GL042798

Ropelewski CF, Halpert MS (1987) Global and regional scale precipitation patterns associated with the El Nino/Southern Oscillation. Mon Weather Rev 115:1606–1626. doi:10.1175/1520-0493(1987)115<1606:GARSPP>2.0.CO;2

Sano M, Ramesh R, Sheshshayee MS, Sukumar R (2012) Increasing aridity over the past 223 years in the Nepal Himalaya inferred from a tree-ring δ^{18}O chronology. Holocene 22:809–817. doi:10.1177/0959683611430338

Shen CC, Cheng H, Edwards RL, Moran SB, Edmonds HN, Hoff JA, Thomas RB (2003) Measurement of attogram quantities of ^{231}Pa in dissolved and particulate fractions of seawater by isotope dilution thermal ionization mass spectroscopy. Anal Chem 75:1075–1079. doi:10.1021/ac026247r

Shi F, Li J, Wilson RJS (2014) A tree-ring reconstruction of the South Asian summer monsoon index over the past millennium. Sci Rep 4:6739. doi:10.1038/srep06739

Sinha A, Berkelhammer M, Stott L, Mudelsee M, Cheng H, Biswas J (2011) The leading mode of Indian summer monsoon precipitation variability during the last millennium. Geophys Res Lett 38:L15703. doi:10.1029/2011GL047713

Sinha A, Kathayat G, Cheng H, Breitenbach SFM, Mudelsee M, Berkelhammer M, Du Y, Biswas J, Edwards LR (2015) Trends and oscillations in the Indian summer monsoon rainfall over the last two millennia. Nat Commun 6:6309. doi:10.1038/ncomms7309

Stahle DW, Cleaveland M, Therrell M, Gay D, D'arrigo R, Krusic P, Cook E, Allan R, Cole J, Dunbar R (1998) Experimental dendroclimatic reconstruction of the Southern Oscillation. B Am Meteorol Soc 79:2137–2152. doi:10.1175/1520-0477

Tan M (2014) Circulation effect: response of precipitation δ^{18}O to the ENSO cycle in monsoon regions of China. Clim Dyn 42:1067–1077. doi:10.1007/s00382-013-1732-x

Tan L, Cai Y, An Z, Edwards RL, Cheng H, Shen CC, Zhang H (2011) Centennial-to decadal-scale monsoon precipitation variability in the semi-humid region, northern China during the last 1860 years: records from stalagmites in Huangye Cave. Holocene 21:287–296. doi:10.1177/0959683610378880

Tan L, Cai Y, Cheng H, Edwards RL, Shen CC, Gao Y, An Z (2015) Climate significance of speleothem δ^{18}O from central China on decadal timescale. J Asian Earth Sci 106:150–155. doi:10.1016/j.jseaes.2015.03.008

Tao Y, Zhang W, Duan C, Chen Y, Ren J, Xing D, He Q (2014) Climatic causes of continuous drought over Yunnan province from 2009 to 2012. J Yunnan Univ 36:866–874. doi:10.7540/j.ynu.20140312

Thornthwaite CW (1948) An approach toward a rational classification of climate. Geogr Rev 38:55–94. doi:10.2307/210739

Ummenhofer CC, D'arrigo RD, Anchukaitis KJ, Buckley BM, Cook ER (2013) Links between Indo-Pacific climate variability and drought in the Monsoon Asia Drought Atlas. Clim Dynam 40:1319–1334. doi:10.1007/s00382-012-1458-1

Wang B (2006) The Asian monsoon. Springer, Chichester

Wang B, Xiang B, Li J, Webster PJ, Rajeevan MN, Liu J, Ha KJ (2015) Rethinking Indian monsoon rainfall prediction in the context of recent global warming. Nat Commun 6:7154. doi:10.1038/ncomms8154

Webster PJ, Magana VO, Palmer T, Shukla J, Tomas R, Yanai Mu, Yasunari T (1998) Monsoons: processes, predictability, and the prospects for prediction. J Geophys Res Oceans (1978–2012) 103:14451–14510. doi:10.1029/97JC02719

Wernicke J, Griebinger J, Hochreuther P, Brauning A (2015) Variability of summer humidity during the past 800 years on the eastern Tibetan Plateau inferred from δ^{18}O of tree-ring cellulose. Clim Past 11:327–337. doi:10.5194/cp-11-327-2015

Wilson R, Tudhope A, Brohan P, Briffa K, Osborn T, Tett S (2006) Two-hundred-fifty years of reconstructed and modeled tropical temperatures. J Geophys Res 111:C10007. doi:10.1029/2005JC003188

Wu G (2011) Drought in southwest China. Disaster Reduction in China, vol. 1, p 26

Xu H, Hong Y, Hong B (2012) Decreasing Asian summer monsoon intensity after 1860 AD in the global warming epoch. Clim Dyn 39:2079–2088. doi:10.1007/s00382-012-1378-0

Xu H, Yeager KM, Lan J, Liu B, Sheng E, Zhou X (2015) Abrupt Holocene Indian Summer Monsoon failures: a primary response to solar activity? Holocene 25:677–685. doi:10.1177/0959683614566252

Yin H (2010) Droughts in southwest China: how far from drought to catastrophe? South Window 8:54–56

Zhang Q, Li Y (2014) Climatic variation of rainfall and rain day in southwest China for last 48 years. Plateau Meteor 33:372–383. doi:10.7522/j.issn.1000-0534.2013.00032

Zhang P, Cheng H, Edwards RL, Chen F, Wang Y, Yang X, Liu J, Tan M, Wang X, Liu J (2008) A test of climate, sun, and culture relationships from an 1810-year Chinese cave record. Science 322:940–942. doi:10.1126/science.1163965

Zhang X, Zhang X, Guan H, Xie Z (2011) The atmospheric circulation features of the heavy drought in southwest China in autumn 2009. Trop Geogr 31:21–27

Zhang W, Jin FF, Zhao JX, Qi L, Ren HL (2013) The possible influence of a nonconventional El Nino on the severe autumn drought of 2009 in Southwest China. J Clim 26:8392–8405. doi:10.1175/JCLI-D-12-00851.1

Zhao H, Moore GWK (2006) Reduction in Himalayan snow accumulation and weakening of the trade winds over the Pacific since the 1840s. Geophys Res Lett 33:L17709. doi:10.1029/2006GL027339